Environmental Science Nano

ROYAL SOCIETY OF CHEMISTRY

PAPER

View Article Online
View Journal | View Issue

Cite this: *Environ. Sci.: Nano*, 2020, 7, 1464

Toxicogenomics in a soil sentinel exposure to Zn nanoparticles and ions reveals the comparative role of toxicokinetic and toxicodynamic mechanisms†

Marta Novo, *[ab] Elma Lahive,[c] María Díez Ortiz,[cd] David J. Spurgeon[c] and Peter Kille[a]

Received 4th October 2019,
Accepted 20th March 2020

DOI: 10.1039/c9en01124b

rsc.li/es-nano

A critical question for read across of the hazards of nanomaterials is the degree to which their mechanisms of action differ from those of their bulk chemical constituents. It has been established that metal and metal oxide nanoparticles (NPs) can be accumulated by invertebrate species. Moreover, it has been hypothesised that the observed toxicity resulting on exposure to these nanomaterials is most likely to be associated with the releases of ions from external or internal dissolution leading ultimately to toxicity. However, mechanistic confirmation of the similar modes of action for metal oxide nanomaterials and metal ions in studies invertebrates are largely lacking. Therefore, here we present a toxicogenomic study using exposed individuals of the earthworm *Eisenia fetida* from a single genetic lineage. We compared gene expression and pathway responses through RNA-seq analysis at equitoxic concentrations (EC_{50} for reproduction) of ZnO NPs and ionic Zn. We found similar transcriptomic effects for both Zn forms with genetic signatures of tight control of cytosolic Zn concentrations through expression changes of genes encoding several Zn transporters. Activation and regulation of JUN, MAP and JNK kinases indicated a cellular response to the increased Zn concentrations of both forms with compound binding terms also enriched. Our results illustrate the need to consider both toxicokinetic and toxicodynamic mechanisms in the development of adverse outcome pathways for nanomaterials.

Environmental significance

The principal paradigm in nanoecotoxicology currently suggests that the dominant cause of observed toxicity is the uptake and accumulation of the metal ions released following dissolution of pristine NPs. The attribution of the toxicity on metal and metal oxide NPs to their constituent chemicals provides useful read across, as it means that data for the metal itself (ions) can be used to support hazard identification for NPs fabrication. The current study confirms that exposures to the essential metal ion Zn in ion or NPs form results in stimulation of the same cellular pathways, representing a conserved toxicodynamic response, whilst exposure to Zn NP enhances the amplitude of the response by influencing the mechanism of uptake, indicating altered toxicokinetic modality.

1. Introduction

There is growing evidence that metal and metal oxide nanoparticles (NPs) can be accumulated by invertebrate species[1–5] and that, at sufficient exposure concentrations, they can cause toxic effects.[6–11] The dominant paradigm of nanoecotoxicology suggests that it is the uptake and accumulation of the metal ions that are released following the dissolution of the pristine NPs that are the dominant cause of observed toxicity. This reflects that such released metal ions are recognised as being readily available to species for subsequent translocation around the body where they can interact with biomolecules.[12] The attribution of the toxicity on metal and metal oxide NPs to their constituent chemicals

[a] *Organisms and Environment Division, Cardiff School of Biosciences, Cardiff University, Cardiff, CF10 3AT, UK*
[b] *Dpto. Biodiversidad Ecología y Evolución, Facultad de Biología, Universidad Complutense, Jose Antonio Nováis, 12, 28040, Madrid, Spain. E-mail: mnovo@ucm.es, martanovorodriguez@gmail.com*
[c] *UK Centre for Ecology and Hydrology, Maclean Building, Wallingford, Oxfordshire, OX10 8BB, UK*
[d] *LEITAT Technological Center, C/ de la Innovació 2, 08225 Terrassa, Barcelona, Spain*

† Electronic supplementary information (ESI) available. See DOI: 10.1039/c9en01124b

is potentially useful for read across, as it means that data for the metal itself (*e.g.* in ionic form) can be used to support hazard identification for NPs fabricated from that element.[13]

The temporal dynamic of NP dissolution may mean that NP dissolution in the specific exposure medium or on accumulation into the organisms itself cannot proceed to completion over short exposure times typical of many toxicity tests (generally from 1–28 days depending on the tested species). Hence, a common finding from short-term toxicity tests is that NPs cause lower toxic effects than a similar concentration of metals added in a soluble "ionic" form.[14] Longer-term studies over extended time-scales have suggested that with extended incubation time to allow full dissolution, toxic effects can match those of added ions.[15,16] Findings of the key role of dissolution in determining the toxicity of metal and metal oxide NPs suggest that the dominant mechanisms of NP toxicokinetics and toxicodynamics will match those for ionic forms. However, mechanistic evidence for this hypothesis of similar mechanisms of action of NPs and constituent ions is largely lacking, especially in studies with invertebrate species.

Zinc oxides (ZnO) is a class of nanomaterials widely used in product and applications. Uses of ZnO NPs include as UV protector and pigment in cosmetic products including sunscreens, pharmaceuticals, and foods. These applications may result in direct ZnO entry into the environment (*e.g.* through potential use as a fertiliser to address micronutrient Zn deficient[17]) or following release from paints. Further emissions may also occur *via* wastewater streams,[18] wherein they may be chemical transformed (*e.g.* sulphadised, phosphatised[19,20]), before being potentially released to the environment *via* sewage sludge applied to land.[21–23] As an essential element, zinc is required for the normal biology through its role in the cell cycle (mitosis), as enzyme co-factors and in signaling cascades.[24,25] However, Zn supply can also cause toxic effects. Hence, there is a need to better understand the mechanisms through which ZnO NPs interact with soil organisms, including similarity to relatively well studied ionic forms.

The advent of next generation sequencing has allowed nanotoxicogenomic studies to assess the nanomaterial effects through transcriptomics,[9,26,27] including for ZnO NPs. Poynton *et al.*[28] found that ZnO NPs and Zn introduced as a dissolved salt solution (throughout termed "ionic zinc") caused similar gene expression pathway effects for *Hyalella azteca* following exposure at equitoxic concentrations. Landa *et al.*[29] also found a high overlap in the pathway affected by exposure to nano-scale, non-nano "bulk" and ionic Zn in *Arabidopsis thaliana* although 58 significant transcripts were found for the ZnO NPs exposure, most of which were associated with signal transduction and stress response processes. Li *et al.*[30] found both similarities and differences in ZnO NPs and ionic Zn exposed *Mytilus galloprovincialis*. In particular, the ZnO NPs exposure caused effects on apoptosis and the antioxidant system that were not observed in the ionic exposures. Hence, uncertainty remains on the degree of overlap between the mechanisms of effects of ZnO NPs and ionic Zn and as a result in the potential for nano-specific effects.

Earthworms are a valuable model for assessing the mechanisms of action of nanomaterials that may reach the soil environment. In a previous nanotoxicogenomic study for earthworm exposed to Ag NPs and ionic Ag, the main mechanistic difference was associated with differences in expression of genes associated with endocytosis and cilia function. These differences suggest that NPs may be internalised by cells following uptake through these vesicular routes.[9] Given that vesicles are already implied in cellular Zn metabolism, the potential exists for ZnO NPs to undergo direct endocytosis. Such interactions have the potential to affect comparative cellular distribution and concentrations of ZnO NP *versus* ionic form, potentially leading to nanospecific effects. To understand the potential mechanism of action of ZnO NPs compared to ionic Zn toxicity in earthworms, we here undertake a toxicogenomic study in a single genetic lineage of the earthworm *Eisenia fetida*. Gene expression and pathway responses are compared through RNA-seq analysis at a similar effect level (EC_{50} for reproduction) in order to resolve the mechanistic effects of both Zn forms. Our hypothesis is that the toxic effects of ZnO NPs can be attributed to exposure to ionic Zn through NP dissolution and, hence, we expect to find similar transcriptomic pathways effects following exposure to the ZnO NPs and ionic Zn.

2. Methods

2.1. Test medium

The test soil was Lufa 2.2 (LUFA Speyer, Germany) from a batch supplied that had a pH of 5.5 ± 0.2 (mean ± SD) as measured in a 2.5 : 1 0.01 M $CaCl_2$ soil slurry mixture, an organic carbon content measured by furnace combustion at 550 °C of 1.76 ± 0.26 w/w%, a measured cation exchange capacity of 10.2 ± 0.5 meq 100 g^{-1}, and a water holding capacity (WHC) of 42 g per 100 g. The soil was air-dried and <2 mm sieved and 500 g dry weight of soil in a 183 × 120 × 70 mm polypropylene container used for each replicate.

2.2. Experimental animals

Eisenia fetida were obtained from a commercial source (Blades Biological, Kent, UK). All adult and suitably sized (300–600 mg) individuals selected for the study were first confirmed to be a true morphotype *E. fetida* by checking for the clear presence of full striped coloration. All earthworms were initially maintained in culture soil constituting by volume of 33% loamy soil, 33% peat and 33% bark held at 20 ± 1 °C in a 12:12 hour light:dark cycle. During culturing the earthworms were fed excess fresh horse manure to ensure that the earthworms were adults for testing.[31] The manure was free from contamination or medication.

2.3. Chemicals

The ZnO NPs selected for this experiment was NanoSun zinc oxide P99/30 obtained from Microniser Pth Ltd (Dandenong, Australia). NanoSun P99/30 has a near-spherical shape, a nominal average particle size of 30 nm, no coatings or surface modifications and is supplied as a white odourless dry powder of 99.5% purity. These particles were from an identical batch as used by Heggelund *et al.* where full characterisation details can be found (also see Results section).[5] Particles were stored in the dark in a cool, dry place away from any light source and TEM confirmed storage did not change the particles (see Results). In short, the hydrodynamic diameter of the particles in the stock suspension and the zeta potential were determined by dynamic light scattering (DLS) and laser Doppler electrophoresis (LDE) respectively using a Malvern Zetasizer Nano ZS. Density measurements were carried out with a helium pycnometer (Micromeritics AccuPyc, model 1340). Specific surface area (SSA) of powders was measured by Brunauer–Emmett–Teller (BET) method (Micromeritics AccuPyc, model Gemini 2360). Having the specific surface area, and assuming that all particles were spherical and identical, the average diameter of the particles was calculated. X-ray diffraction (XRD) with a Philips X'pert Pro. Diffractometer (PANalytical) was performed to confirm the NPs' crystallographic phase as ZnO.[5] The solid powders were placed in sample holders at room temperature and analyzed with Cu Kα radiation at 2 theta angles from 10 to 100 with 0.03° step. Particle size was determined by Scherrer equation. In addition to the NanoSun ZnO NP and Zn salt reference $Zn(NO_3)_2{\cdot}6H_2O$ (Sigma Aldrich, UK) was used to produce a putative Zn ionic treatment.

2.4. Experimental design and dosing

The toxicity test procedure followed the OECD guideline 222 (earthworm reproduction test *Eisenia fetida/andrei*).[31] Exposure concentrations were 0, 225, 500, 1100, 2200, 4400 mg Zn per kg (DW soil) for the ZnO NPs and 0, 100, 225, 500, 1100, 2200 mg Zn per kg (DW soil) for the ionic Zn. Three replicate containers were used for all Zn treatments and six replicates for the control treatment. All exposures were run concurrently allowing benchmarking against the common control. The ZnO NPs were dosed into the soils directly in the dry powder form. Initially, the amount of powder required was added to a 50 g subsample of the test soil and mixed thoroughly by hand. This aliquot was then added to the remaining soil and mixed to ensure even distribution. An appropriate volume of MilliQ water was then added to increase moisture content to 50% of the soil water holding capacity. To dose the ionic Zn salt treatments, a stock solution of zinc nitrate (nominal concentration 15.13 mg Zn per ml) was added to the test soils and moisture content to 50% of the water holding capacity. Dosed soils were left for one week to allow initial equilibration before the test organisms were introduced.

2.5. Toxicity test procedure

To initiate the experiment, the ten adult, fully-clitellated earthworms were weight as a group (average weight ± SD of 10 earthworms = 5.12 ± 0.42 g) and then added to the soil surface and allowed to burrow into the soil. As food, 10 g dry weight of horse manure wetted to 80% water holding capacity was added to the soil surface in each container. All containers were placed in a controlled temperature room (temperature and photoperiod as above) for a total of 56 days. Over the duration of the test, soils were monitored and any lost water replaced.

After 14 days, the containers were sorted and the numbers of live earthworms counted. Retrieved earthworms were washed, blotted dry and weighed as a batch. The soil was returned to the test containers along with the weighed earthworms and an additional 10 g dry weight of wetted horse manure was added to the soil surface. The containers were maintained for further 14 days. At 28 days exposure, the earthworms were again sorted from the soil and survival and weight recorded. All surviving individuals were then kept on moist filter paper for 24 h to allow them to purge soil from the intestinal tract before snap freezing and storage at −80 °C for later analysis. After adult earthworms were removed, the soils were kept under controlled conditions for a further 28 days to allow juveniles to hatch from laid cocoons. At the end of this period, the containers were placed in a water bath at 60 °C for 15 minutes to heat force any juveniles to the soil surface for easy counting. The counts of juvenile present and the adult survival data were used to calculate reproduction rates (juveniles/earthworm/week).

2.6. Soil pore water pH and soil and earthworm tissues zinc concentration

MilliQ water was added to 25 g dry weight equivalent of soil sampled at 56 days to raise the moisture content to 100% of water holding capacity. One sample was collected per replicate. The saturated soils were left overnight to equilibrate and were centrifuged at 4000*g* through glass wool to collect a pore water sample. This collected pore water for each replicate was pooled to give a single sample per treatment. A subsample of the pore water was ultra-filtered at 10 kDa (Amicon Ultra-15 Filters, Millipore, Ireland) for 1.5 h in order to separate soluble Zn from the nanoparticulate fraction. This ultra-filtered sample was a measure of the soluble Zn in the pore water. These filtered extracts were used for the analysis of soil pH using Sartorius Professional Meter PP-25, Sartorius AG, Goettingen, Germany; combination pH probe, filled with 3 M KCl and total Zn concentration following an established inductively coupled plasma mass spectrometry (ICP-MS) method.[32] Metal concentrations were further also measured in collected soil samples and earthworm tissues (three earthworms per replicate) samples. Approximately 0.75 g of dried soil or 0.5 g of freeze-dried whole earthworm was refluxed with a 3 : 1 mixture of aristar grade hydrochloric and nitric acids at

140 °C for 2.5 h. After digestion, the solutions were allowed to cool and filtered using copper soaked Whatman number 540 (12.5 cm diameter) filter papers. Digests were made up to 50 ml with 0.5% v/v nitric acid and analysed by ICP-MS using a Perkin Elmer Nexion 300D instrument.

2.7. Worms for transcriptome analysis

Earthworms from the exposure concentration closest to $EC_{50_{reproduction}}$ values for ZnO NPs and ionic Zn were used for the transcriptome analyses. Stored individuals were initially crushed under liquid nitrogen with a pestle and mortar to provide a powdered tissue sample. A total of 15 individuals per selected treatment were genotyped (five per replicate as shown in ESI† File S1) to ensure that only earthworms from the same lineage were taken forward for full RNAseq analysis. Genotyping was conducted using DNA extracted from 25 mg of tissue using the DNAeasy Tissue Kit (QIAGEN) protocol. A fragment of the mitochondrial gene cytochrome c oxidase subunit I (COI) was amplified using the primers LCO1490 and HCO2198[33] following Novo *et al.*.[9] Sequences were aligned in CLUSTALX v. 2.0.12.[34] Haplotypes were retrieved in DNAcollapser[35] and compared to those from Novo *et al.*[9] Earthworms from the same lineage of *Eisenia fetida* were selected for RNA extraction in next step (see haplotypes in S1† and their location within a phylogenetic tree in Novo *et al.*[9]).

Transcriptomes were generated for ZnO NPs and ionic Zn exposed genotyped individuals from each true biological replicate container for the exposure concentration closest to the respective $EC_{50_{reproduction}}$ and also the control (one earthworm per replicate, three replicates per treatment, except in one case, see S1†). RNA was extracted from 50 mg aliquot of powdered tissue of each selected individual by combined extraction in 1.5 ml of Trizol and column purification approach using RNeasy mini kit (QIAGEN) as described in Novo *et al.*[9] RNA integrity was verified using Bioanalyzer (RNA Nano Chip) and was sent to BaseClear (www.baseclear.com) for library preparation and transcriptome sequencing. Ten libraries were prepared and multiplexed following Tru-Seq (Illumina) protocol and sequenced on Illumina Hi-Seq 2000 using a 50 cycle single-ended protocol designed to yield a minimum of 20 million reads per sample. The data was checked for base quality and filtered for data passing the Illumina chastity default parameters. Sequences containing adapters and/or PhiX control signal were removed using a BaseClear filtering protocol.

2.8. Data analysis

2.8.1. Bioassay data and tissue metal concentrations. Data for survival and reproduction were first checked for normal variance structure using Anderson–Darling normality test. Concentration specific effects on reproduction (juvenile production rates) were analysed for each of the separate zinc types using one-way analysis of variance (ANOVA). Where significant differences were found, the Tukey test was used to identify significant differences between treatments and the control (Minitab 16) as this allowed identification of difference both against controls and between different treatment concentrations. LC_{50} values for survival were calculated using probit analysis (Minitab 16). Data for reproduction (juvenile production rate) was used for least square fitting of a three parameter log logistic model (eqn (1)) to obtain estimate EC_{50} values with standard errors in SigmaPlot 13.0.

$$y = y_{max}/(1 + (c/EC_{50})\exp(b)) \quad (1)$$

where y_{max} is the upper asymptote, c is concentration in soil/pore water/earthworm, EC_{50} is the concentration resulting in a 50% effect on the measured endpoint and b the slope parameter. For the analysis of survival data, a binominal distribution of data within each treatment was assumed. All concentration-response relationships were fitted using total soil Zn concentration.

2.8.2. Quantitative transcriptomic analysis. Sequence reads (50 bp) generated from the 10 exposure samples were mapped against the reference transcriptome of *E. fetida* available from Novo *et al.* (2015), annotated against Swissprot, using Bowtie1[36] allowing three mismatches (–v 3) and retrieving only uniquely mapped reads (m –1). EdgeR was selected for statistical analyses.[37] Some contigs were removed for subsequent analyses where the observed frequency of mapped reads per million fell below 1 for all the replicates within a specific group. The data analysis workflow followed Novo *et al.*[9] Exact tests were completed for each of the comparisons (*i.e.* NP *vs.* control; ion *vs.* control; NP *vs.* ion) and the differentially expressed transcripts identified ($P < 0.05$) were further used to perform enrichment analyses in DAVID.[38] Cytoscape 2.8.2[39] was used for visualization and interpretation of the enrichment analyses using the plugin Enrichment Map v 1.2[40] with default settings (*p*-value Cutoff 0.005, FDR *Q*-value Cutoff 0.1). Top enrichment terms in David (FDR <10) were visualized in REViGO.[41]

3. Results

3.1. Particle characterisation

These particles were from an identical batch as used by Heggelund *et al.* where full characterisation details can be found (also see ESI†).[5] In brief, TEM indicate that the particles were spherical and relatively monodispersed (figure in ESI† File S2). The average primary particle diameter of the ZnO material was 29.8 ± 9.4 nm (mean ± standard deviation). Crystallite size measurements *via* XRD, specific surface area and grain size from BET and zeta-potential and density measurements are all reported in table in ESI† File S2.

3.2. Soil pore water zinc concentrations and pH

The concentration of Zn in the pore water increased with increasing total Zn concentration in the soil. The

concentration of Zn in the pore water was higher in the ZnO NP dosed soils compared to the ionic Zn dosed soils but up to 400 times at 2200 mg kg^{-1} exposure concentration. The difference between total Zn in the pore water and the ultra-filtered pore water was small or equivalent indicating that all the zinc in the pore water was in the soluble form.

Increasing concentration of ZnO NP in the soil resulted in the pH to increase from 6.16 in the control to 7.39 at the highest exposure concentration, 4400 mg kg^{-1}. Conversely, increasing concentration of ionic Zn in the soil decreased soil pH from 6.16 to 5.84 at 2200 mg kg^{-1} (ESI† File S3).

3.3. Earthworm survival, reproduction and Zn body concentrations

After 28 days, there was >93% survival (ESI† File S4) of *E. fetida* in soil spiked with ZnO NPs at concentrations up to 4400 mg Zn per kg and so no LC_{50} could be calculated. In the ionic Zn exposure, 100% survival in all treatments up to 225 mg kg^{-1}, 97% survival at 500 mg Zn per kg and all earthworms exposed to 1100 mg Zn per kg and above died. The calculated LC_{50} was 608 mg Zn per kg. Reproduction was reduced in a dose-dependent manner on exposure to both Zn forms (ESI† File S5). Calculated EC_{50} values of 693 ± 135.8 and 374 ± 72 mg Zn per kg were estimated for ZnO NPs and ionic Zn, respectively. The treatment closest to these EC_{50} values that were selected for use in the transcriptome assessment were 500 ZnO mg Zn per kg and 225 mg Zn per kg for the ionic Zn. Juvenile production in these treatments corresponded to levels at 64.2% and 89.2% of control values. The mean body concentrations (±SD, ESI† File S4) of the control earthworms was 102 ± 4 mg Zn per kg, excluding a single extreme outline value (mean 154 mg Zn per kg including outlier). Tissue Zn concentrations in *E. fetida* exposed to 225 and 500 mg Zn per kg were 120 ± 0.6 mg Zn per kg and 140 ± 2 mg Zn per kg for the ZnO exposure and 142 ± 7 mg Zn per kg and 153 ± 5 mg Zn per kg for the ionic Zn treatments. At the two concentrations selected for the RNA-seq analysis (500 mg and 225 mg Zn per kg for the ZnO and ionic Zn forms) internal concentration did not differ significantly (*T*-test, $p > 0.05$).

3.4. Differential expression analyses

Reads have been submitted to the European eucleotide archive (ENA) under study number PRJEB7953. In ESI† File S1 information on numbers of reads per sample and mapping is presented. Between 26 and 49 million reads were generated per sample. Around 75% of the reads from each sample mapped against the reference transcriptome, and 49% of the reads uniquely mapped and, therefore, were informative for subsequent quantitative analyses. Paired comparisons ($P < 0.05$ in EdgeR) of; (i) Zn ion *vs.* control yielded 1590 differentially expressed (DE) contigs, 347 of which gave a hit in Swissprot of which 317 were non-redundant hits; (ii) ZnO NPs *vs.* control resulted in 1972 DE transcripts, 472 with a Swissprot hit of which 397 were non-redundant; and (iii) ZnO NP *vs.* Zn ion showed 2043 DE contigs, 455 with hit and 394 non-redundant. The Venn diagram in Fig. 1 shows the overlap of DE contigs with non-redundant hits among the pairwise treatment comparisons. There were 130 common non-redundant DEs for Zn NPs and ions comparisons to control. The full list of differentially expressed genes and enrichment analyses in DAVID are shown in Supplementary Files S6 and S7† respectively and REViGO analyses in S8.†

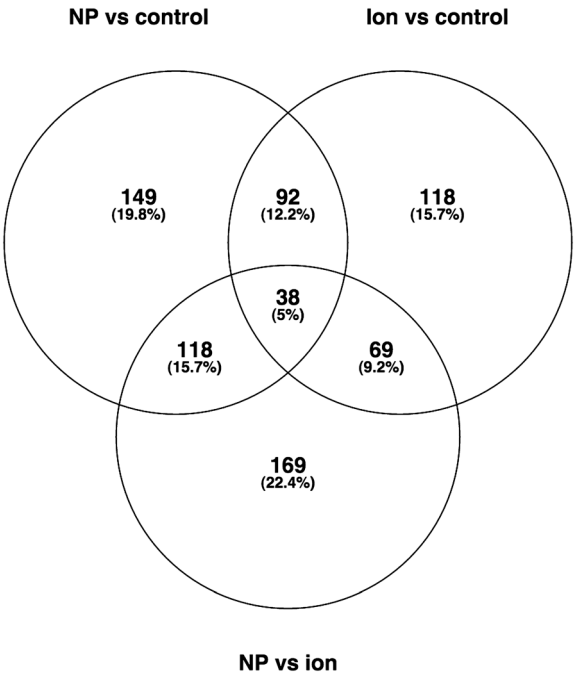

Fig. 1 Venn diagram indicating the number of overlapping differentially expressed genes ($P < 0.05$ in EdgeR) among the three comparisons. Only transcripts with blast hit are included.

3.5. Different transcriptional effects of ZnO NP and Zn ion exposures

As shown by cytoscape network presented in Fig. 2A, significantly enriched pathways when comparing Zn NPs *versus* ions exposure related to vesicular/membrane transport, compound binding, extracellular region, adhesion and peptidases (see in Table 1 enrichment terms corresponding to the nodes in Fig. 2A). A number of distinct pathways are related to vesicular/membrane transport those that show the most discrete changes between ion and NPs include the dynein complex, brush border, apical part of the cell, apical plasma membrane and lipoprotein transport (Table 1). Several dynein heavy chains were DE and specifically dynein heavy chain 5, part of a microtubule-associated motor protein complex, was one of the most upregulated genes in this comparison (NPs *vs.* ions), also appearing in the list of top downregulated for the Zn ion *vs.* control comparison (Table 2). Caltractin, which plays a fundamental role in the

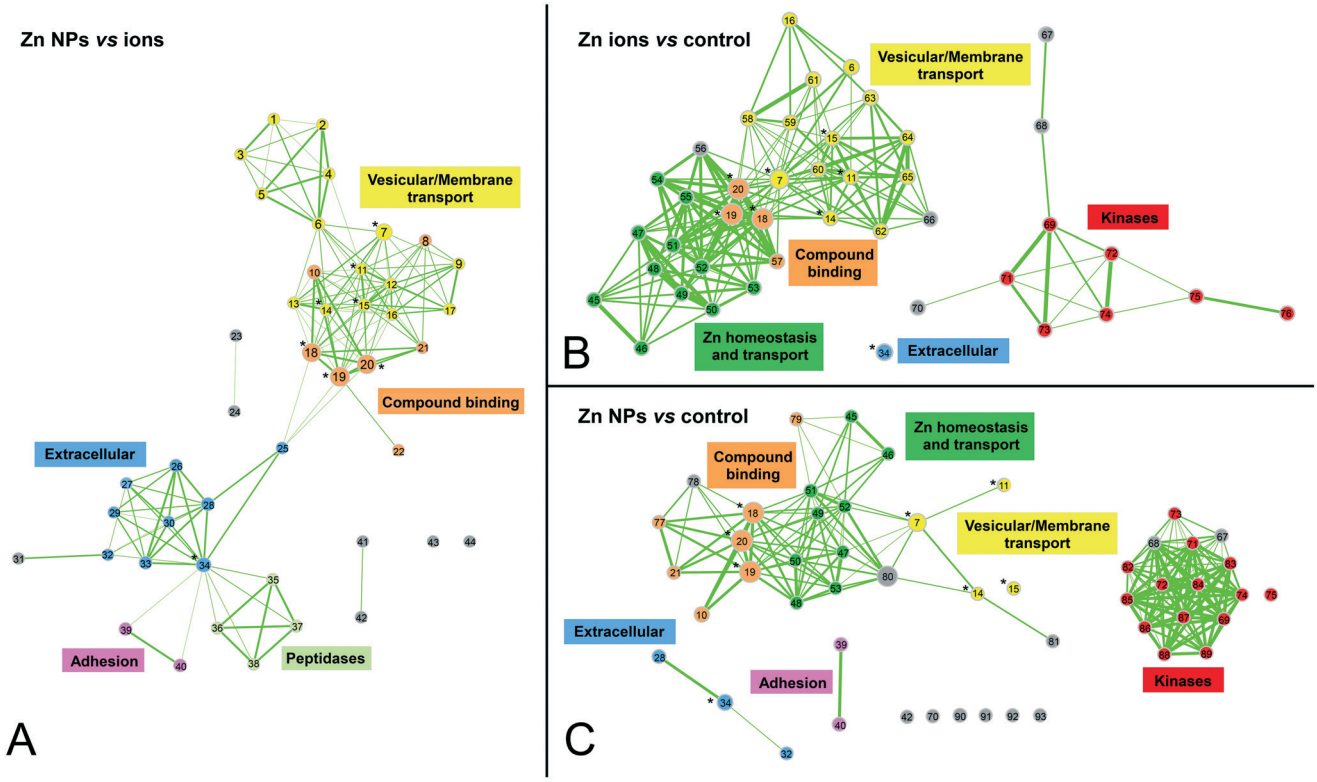

Fig. 2 Go-term networks generated by cytoscape (*P*-value Cutoff 0.005, FDR Q-value Cutoff 0.1) after enrichment analyses in DAVID (*P*-value 0.05). Go-terms are represented by numbers in the nodes and are shown in Tables 1 and 3. Node size is related to number of genes implicated in that term (see ESI† File S7). Numbers highlighted with asterisks are common nodes in the three comparisons. A: comparison NPs *versus* ions; B: ions *versus* control; C: NPs *versus* control.

structure and function of the microtubule-organizing center, was one of the top downregulated for NPs (both in NPs *vs.* ions and NPs *vs.* control comparisons, Table 2). Within the compound binding term, ion binding, tetrapyrrole binding, and calcium ion binding were the most enriched terms in NPs *vs.* ions comparison (Table 1). Several Zn finger proteins (26, 62, 92, 625, 778) were downregulated for the ZnO NPs *vs.* ionic Zn comparison, as well as Zn carboxipeptidase, ovochymase, and several forms of cytochrome P450 (see ESI† File S6). Sarcoplasmic calcium-binding protein was one of the top upregulated for NPs (both in NPs *vs.* ions and NPs *vs.* control comparisons) and top downregulated for ions *vs.* control (Table 2). A Zinc transporter protein, ZIP10, was downregulated for the comparison NPs *vs.* ions. ZIP 10 was a top downregulated gene in the ZnO NPs *vs.* control comparison and was also downregulated for Zn ion *vs.* control, albeit to a lesser extent (Tables 2 and 4). This means that while being downregulated for both NPs and ions *vs.* control, ZIP10 downregulation was higher for NPs.

Within the extracellular region and cell and biological adhesion terms, agrin, which plays a key role in cell surface organisation (especially in neurons) and is also implicated in cytoskeleton organisation, was one of the most downregulated genes following ZnO NPs exposure when compared to the Zn ion treatment and the control (see Table 2). ZnO NPs exposure also resulted in >3 fold downregulation compared to Zn ion exposure for lysozyme, collagen alpha-1 (XII), Chymotrypsin like serine proteinase and neural cell adhesion molecule 2, a surface-expressed glycoprotein with a role in cell adhesion. Uromodulin, matrilin, laminin, fibropellin, and several von Winderbrand factors were also downregulated for this comparison to a lesser extent, in some cases also being top regulated genes for the NP or ions *vs.* control comparisons (Table 2). SCO-spondin, a novel relative of the thrombospondin family involved in cell aggregation, also shows ~ 3 fold downregulation in the NPs *vs.* ions exposure (File S6†). Finally, a number of TNF genes were differentially regulated by the ZnO and Zn ion exposure. For example, TNF receptor-associated factor 3 was differentially regulated by the two forms being downregulated in the ion *vs.* control comparison and unchanged following ZnO exposure (Table 2 and File S6†).

3.6. Shared effects after exposure to ZnO NPs and ionic Zn when compared to control

Enriched pathways after exposure to both ZnO NPs and ionic Zn compared to controls are shown as networks in Fig. 2B and C; the main enriched GO terms in Table 3 and a list of common DE expressed hits for both comparisons is shown in Table 4. Complete lists of differentially expressed genes and enriched analyses are detailed in ESI† S6 and S7,

Table 1 Enrichment results from DAVID for the comparison NPs *versus* ions. Only enrichment terms with *P* values < 0.05 are shown, those with FDR < 10 are shown in bold. See complete results of the enrichment analyses in ESI† File S7 and complete gene lists in S6.† See Fig. 2A for correspondence of numbers within networks nodes. BP: biological process, MF: molecular function, CC: cellular component

		NPs *versus* ion		
Node	Term	Category	*P* value	Fold enrichment
VESICULAR/MEMBRANE TRANSPORT				
1	GO:0001539 ~ ciliary or flagellar motility	BP	0.007	9.92
2	GO:0005930 ~ axoneme	CC	0.011	4.40
3	GO:0005858 ~ axonemal dynein complex	CC	0.028	11.19
4	GO:0044463 ~ cell projection part	CC	0.022	2.29
5	**GO:0030286 ~ dynein complex**	**CC**	**0.006**	**5.03**
6	GO:0042995 ~ cell projection	CC	0.040	1.57
7	GO:0005886 ~ plasma membrane	CC	0.009	1.31
9	GO:0005764 ~ lysosome	CC	0.025	2.25
11	**GO:0005903 ~ brush border**	**CC**	**0.001**	**7.04**
12	GO:0005905 ~ coated pit	CC	0.027	4.37
13	**GO:0045177 ~ apical part of cell**	**CC**	$\mathbf{2.20 \times 10^{-4}}$	**3.94**
14	**GO:0016324 ~ apical plasma membrane**	**CC**	$\mathbf{3.76 \times 10^{-4}}$	**4.46**
15	GO:0006898 ~ receptor-mediated endocytosis	BP	0.007	6.38
16	**GO:0042953 ~ lipoprotein transport**	**BP**	$\mathbf{2.09 \times 10^{-4}}$	**29.76**
17	GO:0000323 ~ lytic vacuole	CC	0.027	2.21
COMPOUND BINDING				
8	GO:0031419 ~ cobalamin binding	MF	0.017	14.40
10	**GO:0005509 ~ calcium ion binding**	**MF**	$\mathbf{1.45 \times 10^{-4}}$	**1.87**
18	GO:0046872 ~ metal ion binding	MF	0.045	1.15
19	**GO:0043167 ~ ion binding**	**MF**	**0.006**	**1.22**
20	GO:0043169 ~ cation binding	MF	0.022	1.18
21	**GO:0046906 ~ tetrapyrrole binding**	**MF**	**0.004**	**2.95**
22	GO:0031404 ~ chloride ion binding	MF	0.034	3.32
EXTRACELLULAR				
25	GO:0005615 ~ extracellular space	CC	0.018	2.14
26	**GO:0031012 ~ extracellular matrix**	**CC**	$\mathbf{3.60 \times 10^{-5}}$	**2.89**
27	GO:0005604 ~ basement membrane	CC	0.010	3.78
28	**GO:0044421 ~ extracellular region part**	**CC**	$\mathbf{2.98 \times 10^{-6}}$	**2.52**
29	**GO:0005201 ~ extracellular matrix structural constituent**	**MF**	$\mathbf{2.40 \times 10^{-5}}$	**6.35**
30	**GO:0044420 ~ extracellular matrix part**	**CC**	**0.002**	**3.57**
32	**GO:0043062 ~ extracellular structure organization**	**BP**	**0.004**	**3.01**
33	**GO:0005578 ~ proteinaceous extracellular matrix**	**CC**	$\mathbf{2.18 \times 10^{-5}}$	**2.99**
34	**GO:0005576 ~ extracellular region**	**CC**	$\mathbf{2.31 \times 10^{-7}}$	**2.11**
PEPTIDASES				
35	**GO:0004857 ~ enzyme inhibitor activity**	**MF**	**0.007**	**2.94**
36	GO:0004866 ~ endopeptidase inhibitor activity	MF	0.010	3.83
37	**GO:0030414 ~ peptidase inhibitor activity**	**MF**	**0.001**	**4.27**
38	**GO:0004867 ~ serine-type endopeptidase inhibitor activity**	**MF**	**0.002**	**5.12**
ADHESION				
39	**GO:0007155 ~ cell adhesion**	**BP**	$\mathbf{6.35 \times 10^{-4}}$	**2.13**
40	**GO:0022610 ~ biological adhesion**	**BP**	$\mathbf{6.65 \times 10^{-4}}$	**2.13**
OTHERS				
23	GO:0006040 ~ amino sugar metabolic process	BP	0.033	10.30
24	GO:0009254 ~ peptidoglycan turnover	BP	0.044	44.64
31	GO:0050808 ~ synapse organization	BP	0.016	4.06
41	GO:0051147 ~ regulation of muscle cell differentiation	BP	0.049	4.83
42	GO:0007009 ~ plasma membrane organization	BP	0.048	8.37
43	GO:0009986 ~ cell surface	CC	0.044	2.03
44	GO:0048608 ~ reproductive structure development	BP	0.041	3.15

and REViGO analyses for individual comparisons *versus* control and for common hits in S8.† The main commonly affected processes following exposure to both Zn forms were related to Zn homeostasis and transport; compound binding; extracellular matrix; vesicular/membrane transport and kinases. The occurrence of some of these high level terms such as vesicular/membrane transport, compound binding or extracellular region in both differential and shared response reflects both the diversity of pathways within them (specially vesicular/membrane transport) but also that some lower level terms present a varied degree of response, making them significantly enriched for all the comparisons. Regarding the Zn homeostasis related pathways, several terms including Zn homeostasis itself and also transport and transmembrane transporter activity were enriched in the DE gene lists (Table 3). Several specific Zn transporters were differentially expressed. These included ZIP10, ZIP4, and Zn transporter foi (closely related to ZIP6) which were downregulated by

Table 2 The self-assembly process of CHA microspheres in the presence of Na_2EDTA and urea under hydrothermal homogeneous precipitation route.

Zn NPs *vs.* ions		Zn ions *vs.* control		Zn NPs *vs.* control	
Up-regulated	Down-regulated	Up-regulated	Down-regulated	Up-regulated	Down-regulated
Alanyl-tRNA editing protein Aarsd1-B	Agrin	Polyadenylate-binding protein 1	Sarcoplasmic calcium-binding protein	Lysenin-related protein 3	Protein Star
Exostosin-1	Caltractin	Myosin-10	Probable G-protein coupled receptor 158	Mitogen-activated protein kinase kinase kinase	UDP-galactose:fucoside alpha-3-galactosyltransferase
Poly [ADP-ribose] polymerase 14	Cell cycle control protein 50A	Tripartite motif-containing protein 2	Dynein heavy chain 5	Polyadenylate-binding protein 1	Caltractin
Sarcoplasmic calcium-binding protein	Chymotrypsin-like serine proteinase	Immunoglobulin superfamily DCC subclass member 4	Poly [ADP-ribose] polymerase 14	Tripartite motif-containing protein 2	Major surface trophozoite antigen 11
Probable G-protein coupled receptor 158	Collagen alpha-1(XII) chain	Mitogen-activated protein kinase kinase kinase 9	Alanyl-tRNA editing protein Aarsd1-B	Filamin-C	ETS homologous factor
Dynein heavy chain 5	ETS homologous factor	Protein kinase C and casein kinase substrate in neurons protein 2	Pancreatic secretory granule membrane major glycoprotein GP2	Exostosin-1	Pancreatic secretory granule membrane major glycoprotein GP2
Synaptogyrin-2	Fucose mutarotase	O-Acetyl-ADP-ribose deacetylase MACROD1	TNF receptor-associated factor 3	Exostosin-1c	Chymotrypsin-like serine proteinase
TNF receptor-associated factor 3	Lysozyme	O-Acetyl-ADP-ribose deacetylase MACROD2	Protein Star	Myosin-10	Zinc transporter ZIP10
Filamin-C	Major surface trophozoite antigen 11	Filamin-C	Synaptogyrin-2	Immunoglobulin superfamily DCC subclass member 4	Neural cell adhesion molecule 2
Perlucin-like protein	Neural cell adhesion molecule 2	Mitogen-activated protein kinase kinase kinase 10	Intermediate filament protein B	Mitogen-activated protein kinase kinase kinase 9	Fucose mutarotase
Ras and EF-hand domain-containing protein	Nucleolar GTP-binding protein 1	Long-chain fatty acid transport protein 4	Multiple epidermal growth factor-like domains protein 10	Protein kinase C and casein kinase substrate in neurons protein 2	Sushi
Spherulin-2A	Protein Star	Degenerin unc-8	Serine/threonine-protein kinase unc-51	O-Acetyl-ADP-ribose deacetylase MACROD1	Serine/threonine-protein kinase unc-51
	Putative uncharacterized protein DDB_G0282499	Angiopoietin-4		Degenerin unc-8	Agrin
	Retrovirus-related Pol polyprotein from transposon 17,6	von Willebrand factor D and EGF domain-containing protein		O-Acetyl-ADP-ribose deacetylase MACROD2	Chymotrypsin inhibitor
	Sushi	Sarcoplasmic calcium-binding protein		Long-chain fatty acid transport protein 4	Retinol dehydrogenase 7
	Synaptogyrin-2	Fibropellin-1		Saccharopine dehydrogenase-like oxidoreductase	Zinc finger protein 62
	UDP-galactose:fucoside alpha-3-galactosyltransferase	Quinone oxidoreductase-like protein 2		Antistasin	Palmitoyl-protein thioesterase 1
	Uncharacterized protein U88	Exostosin-1c		Arginase-1	von Willebrand factor A domain-containing protein 5A
	Zinc carboxypeptidase A 1	Phytanoyl-CoA hydroxylase-interacting protein-like		Sarcoplasmic calcium-binding protein	von Willebrand factor D and EGF domain-containing protein
	Zinc finger protein 62			Lysine-specific demethylase 5A	von Willebrand factor D and EGF domain-containing protein
	Zinc finger protein 778			Myosin essential light chain	Uromodulin

Table 2 (continued)

Zn NPs *vs.* ions		Zn ions *vs.* control		Zn NPs *vs.* control	
Up-regulated	Down-regulated	Up-regulated	Down-regulated	Up-regulated	Down-regulated
				Mitogen-activated protein kinase kinase kinase 10	Glutamyl aminopeptidase
				Fibropellin-1	Lactase-like protein
				Poly(ADP-ribose) glycohydrolase ARH3	Putative uncharacterized protein DDB_G0282499
				BTB/POZ domain-containing protein 6-A	Collagen alpha-1(XII) chain
				Dual specificity tyrosine-phosphorylation-regulated kinase 1A	Golgin subfamily A member 2
				Multidrug resistance-associated protein 1	Clustered mitochondria protein homolog
				Palmitoyl-protein thioesterase 1	
				Probable RNA-directed DNA polymerase from transposon BS	

both ZnO NPs and ionic Zn exposure; ZIP3 and ZIP12 downregulated only for the ZnO NPs and Zn transporter 1 which was upregulated for both Zn forms (Table 4 and S6†). DE genes related to compound binding, extracellular matrix, adhesion and vesicular/membrane transport were already mentioned in the previous section. One of the top downregulated genes for ions was Multiple epidermal growth factor-like domains protein 10 that may play a role in cell adhesion and motility. For comparison of ions *vs.* control, some terms related to vesicles are enriched as well. Kinases, categorised under terms related to activation and regulation of JUN, MAP, and JNK were significantly enriched for both Zn forms (Table 3), some mitogen-activated protein kinases were also upregulated as well as some protein kinase CK2 (File S6†). These pathways are more impacted by the ZnO NPs than for the ionic Zn as shown by the higher number of terms enriched for the former exposure (Table 3, nodes in the network Fig. 2B and C).

Separate enrichment analyses were conducted for both the up and down regulated DE genes for the ZnO NP and ion *vs.* control comparisons (see ESI† File S8 for REViGO graphics). Those highlighted the downregulation of Zn ion transmembrane transport (including ZIP10, ZIP4 and Zn transporter foi), membrane-bounded and cytoplasmic vesicles, ATP binding and protein, tyrosine kinase activity. Regulation of intracellular signal transduction, protein autophosphorylation, metal ion transport, Zn ion transmembrane transport (including Zn transporter 1 and Zn/Cd resistance protein), urea metabolism, plasma membrane, extracellular region, JUN kinase activity and protein homodimerization activity were all terms represented in the upregulated gene lists.

4. Discussion

Earthworms show moderate sensitivity to Zn, as illustrated by our own and the results of other,[42,43] with $EC_{50_{reproduction}}$ values in the range 200–600 mg Zn per Kg depending on the earthworm species tested and soil type.[42–44] The median Zn concentrations for 1083 soils measured in the UK was 61.5 mg Zn per kg,[45] suggesting that the window of essentiality between potential deficiency and toxicity for Zn may be relatively small for earthworms. The effects of long-term metal aging in polluted soils in the field have been found to reduce metal bioavailability, which in part may mitigate the potential ecotoxicological hazard of Zn. However, even with aging potentially reducing risk, zinc remains one of the chemical most likely to expert toxic effects in soils and freshwater systems.[46–48] Given the potential high ranking of risk associated with Zn pollution, it is highly relevant to review the effects of this metal in nanomaterial forms, given the relatively large amounts of ZnO NP produced and used annually worldwide.

We found that ionic Zn was more toxic compared to ZnO NPs. For earthworms exposed to the ionic Zn, survival and reproduction were impacted at lower concentrations, almost half compared to ZnO NPs having the same level of effect. This is in agreement with previous studies that have also

Table 3 Enrichment results from DAVID for the comparisons of NPs and ions *vs.* control. Only enrichment terms with *P* values < 0.05 are shown, those with FDR < 10 are shown in bold. See complete results of the enrichment analyses in ESI† File S7 and complete gene lists in S6.† See Fig. 2B and C for correspondence of numbers within networks nodes. BP: biological process, MF: molecular function, CC: cellular component

			Ions *versus* control		NPs *versus* control	
Node	Term	Category	*P* value	Fold enrichment	*P* value	Fold enrichment
Common with comparison NPs *vs.* ions						
VESICULAR/MEMBRANE TRANSPORT						
6	GO:0042995 ~ cell projection	CC	0.045	1.64	No	No
7	GO:0005886 ~ plasma membrane	CC	**0.001**	**1.44**	0.009	1.30
10	GO:0005509 ~ calcium ion binding	MF	No	No	**0.001**	**1.72**
11	GO:0005903 ~ brush border	CC	**4.68×10^{-4}**	**9.02**	0.011	5.67
14	GO:0016324 ~ apical plasma membrane	CC	0.030	3.43	0.028	3.02
15	GO:0006898 ~ receptor-mediated endocytosis	BP	**3.86×10^{-4}**	**9.42**	0.045	4.98
16	GO:0042953 ~ lipoprotein transport	BP	**0.005**	**27.48**	No	No
COMPOUND BINDING						
18	GO:0046872 ~ metal ion binding	MF	0.043	1.17	**0.007**	**1.21**
19	GO:0043167 ~ ion binding	MF	0.034	1.18	**0.001**	**1.25**
20	GO:0043169 ~ cation binding	MF	0.047	1.17	**0.002**	**1.25**
21	GO:0046906 ~ tetrapyrrole binding	MF	No	No	**1.21×10^{-4}**	**3.64**
EXTRACELLULAR						
28	GO:0044421 ~ extracellular region part	CC	No	No	0.038	1.60
32	GO:0043062 ~ extracellular structure organization	BP	No	No	0.034	2.41
34	GO:0005576 ~ extracellular region	CC	**0.004**	**1.67**	**4.14×10^{-4}**	**1.84**
ADHESION						
39	GO:0007155 ~ cell adhesion	BP	No	No	0.017	1.75
40	GO:0022610 ~ biological adhesion	BP	No	No	0.017	1.74
OTHERS						
42	GO:0007009 ~ plasma membrane organization	BP	No	No	**0.005**	**10.89**
Only for comparisons to control						
ZN HOMEOSTASIS AND TRANSPORT						
45	GO:0006882 ~ cellular zinc ion homeostasis	BP	**0.006**	**23.55**	0.010	18.67
46	GO:0055069 ~ zinc ion homeostasis	BP	0.008	20.61	0.013	16.34
47	GO:0046915 ~ transition metal ion transmembrane transporter activity	MF	**0.003**	**8.39**	**8.74×10^{-4}**	**7.85**
48	GO:0006829 ~ zinc ion transport	BP	**7.05×10^{-4}**	**11.95**	**9.79×10^{-6}**	**13.26**
49	GO:0005385 ~ zinc ion transmembrane transporter activity	MF	**7.17×10^{-5}**	**20.66**	**1.89×10^{-4}**	**16.10**
50	GO:0000041 ~ transition metal ion transport	BP	0.020	4.82	**2.99×10^{-4}**	**6.12**
51	GO:0006812 ~ cation transport	BP	0.017	1.90	0.033	1.69
52	GO:0030001 ~ metal ion transport	BP	**0.006**	**2.19**	0.022	1.85
53	GO:0015082 ~ di-. tri-valent inorganic cation transmembrane transporter activity	MF	**0.002**	**6.45**	**0.007**	**5.02**
54	GO:0031420 ~ alkali metal ion binding	MF	0.025	2.37	No	No
55	GO:0022890 ~ inorganic cation transmembrane transporter activity	MF	0.019	2.92	No	No
VESICULAR/MEMBRANE TRANSPORT						
58	GO:0031982 ~ vesicle	CC	**0.006**	**1.97**	No	No
59	GO:0031526 ~ brush border membrane	CC	**0.004**	**12.38**	No	No
60	GO:0030139 ~ endocytic vesicle	CC	**0.005**	**5.35**	No	No
61	GO:0031410 ~ cytoplasmic vesicle	CC	**0.008**	**1.95**	No	No
62	GO:0016044 ~ membrane organization	BP	0.044	1.95	No	No
63	GO:0016192 ~ vesicle-mediated transport	BP	0.047	1.71	No	No
64	GO:0010324 ~ membrane invagination	BP	**0.006**	**2.80**	No	No
65	GO:0006897 ~ endocytosis	BP	**0.006**	**2.80**	No	No
KINASES						
69	GO:0004706 ~ JUN kinase kinase kinase activity	MF	**0.007**	**23.02**	**4.35×10^{-4}**	**23.91**
71	GO:0010627 ~ regulation of protein kinase cascade	BP	0.008	3.46	0.009	3.09
72	GO:0007254 ~ JNK cascade	BP	0.038	5.36	0.014	5.31
73	GO:0046777 ~ protein amino acid autophosphorylation	BP	0.047	3.66	**0.002**	**4.65**
74	GO:0031098 ~ stress-activated protein kinase signaling pathway	BP	0.040	5.23	0.015	5.19
75	GO:0004713 ~ protein tyrosine kinase activity	MF	0.022	2.43	**0.007**	**2.46**

Table 3 *(continued)*

Node	Term	Category	Ions *versus* control		NPs *versus* control	
			P value	Fold enrichment	*P* value	Fold enrichment
76	GO:0004715 ~ non-membrane spanning protein tyrosine kinase activity	MF	**0.005**	**5.37**	No	No
82	GO:0004709 ~ MAP kinase kinase kinase activity	MF	No	No	**5.46×10^{-4}**	**8.66**
83	GO:0070302 ~ regulation of stress-activated protein kinase signaling pathway	BP	No	No	0.035	4.03
84	GO:0043506 ~ regulation of JUN kinase activity	BP	No	No	0.023	6.45
85	GO:0007257 ~ activation of JUN kinase activity	BP	No	No	0.010	8.71
86	GO:0043405 ~ regulation of MAP kinase activity	BP	No	No	0.041	3.15
87	GO:0043507 ~ positive regulation of JUN kinase activity	BP	No	No	0.017	7.26
88	GO:0043408 ~ regulation of MAPKKK cascade	BP	No	No	0.021	3.79
89	GO:0046328 ~ regulation of JNK cascade	BP	No	No	0.033	4.11
COMPOUND BINDING						
57	GO:0031402 ~ sodium ion binding	MF	0.033	2.91	No	No
77	GO:0020037 ~ heme binding	MF	No	No	**2.72×10^{-4}**	**3.58**
79	GO:0046870 ~ cadmium ion binding	MF	No	No	0.047	41.85
OTHERS						
56	GO:0006814 ~ sodium ion transport	BP	0.045	2.69	No	No
66	GO:0006766 ~ vitamin metabolic process	BP	0.047	3.66	No	No
67	GO:0046983 ~ protein dimerization activity	MF	0.023	2.07	0.031	1.86
68	GO:0042803 ~ protein homodimerization activity	MF	0.011	2.73	0.019	2.34
70	GO:0009967 ~ positive regulation of signal transduction	BP	0.037	2.56	0.044	2.28
78	GO:0009055 ~ electron carrier activity	MF	No	No	0.018	2.14
80	GO:0031224 ~ intrinsic to membrane	CC	No	No	0.046	1.15
81	GO:0031430 ~ M band	CC	No	No	0.025	11.90
90	GO:0004175 ~ endopeptidase activity	MF	No	No	0.022	1.84
91	GO:0030545 ~ receptor regulator activity	MF	No	No	0.043	8.97
92	GO:0006955 ~ immune response	BP	No	No	0.026	2.23
93	GO:0033692 ~ cellular polysaccharide biosynthetic process	BP	No	No	0.036	5.45

shown lower toxicity for nano-forms when compared to ionic forms of the same metals.[5,9,14,49] The reasons for the lower toxicity of ZnO NPs compared to the ionic form has previously been attributed to slow dissolution of ions from the ZnO NPs and so lower exposure and reduced Zn availability to the organisms when exposed as NPs compared to when added in ionic form.[5,50–52] Hence, the lower toxicity of the ZnO NPs compared to ionic Zn found in this study may be associated with lower bioavailability due to dissolution limitation. In this study, the pore water concentrations measured in the ionic exposure were higher compared to soils spiked with ZnO NPs by up to 400 times. However, ultra-filtering the pore waters did not reduce the Zn concentration, indicating that the ZnO NPs in the pore water were in the soluble form. So although there was ionic Zn available in the ZnO NP exposure, the exposure to ionic Zn was higher in the ionic Zn dosed soils compared to the ZnO NPs explaining to some extent the lower toxicity observed in the ZnO NPs, in agreement with other similar studies.[5,50–52] However the difference in sensitivity between the two Zn forms is not 400 fold (closer to 2-fold) suggesting another exposure route besides pore water. Earthworms also ingest soil and so are also exposed to Zn associated with the soil solid phase. Although the body concentrations were not significantly different at the 225 and 500 mg kg^{-1} exposure concentration, earthworms are known to regulate Zn body concentrations,[53,54] which might explain why we don't see a difference in accumulation between the two Zn forms at the exposure concentrations where there is more limited effect on survival or reproduction. The formation of biogenic particles has also been a suggested mechanism by which earthworms can handle metal exposure, ultimately reducing their exposure to toxic ions.[55] As particles are dissolving it is also possible the earthworms are transforming them to the biogenic forms making the ionic Zn less available and as such lessening toxic pressure.

Measurements of tissue Zn concentrations indicated a slight accumulation in both the ZnO and Zn ion treatments compared to the control (when a single outlier control value was excluded), although not beyond concentrations which would be considered within normal tolerance for earthworm.[53] Given the difference in external exposure concentrations 225 or 500 mg Zn/kg between the control and different Zn treatments, the small magnitude of difference between the control and exposed earthworms indicates either limited uptake and/or active regulation through elimination. Previous studies have indicated a high initial elimination of Zn in *E. fetida*[56] and also *Lumbricus rubellus.*[57] Zn body concentrations in the earthworms exposed to ZnO NPs and ionic Zn did not significantly differ, confirming similar level of internal exposure at the similar levels of reproductive toxicity resulting for both Zn forms.

Table 4 Common differentially expressed genes (EdgeR, *P*-value < 0.05) showing same direction of change (up or down) in both comparisons against control: ions *vs.* control and NPs *vs.* control

Common downregulated Zn NPs and ions *vs.* control		Common upregulated Zn NPs and ions *vs.* control
Adapter protein CIKS	*O*-Acetyl-ADP-ribose deacetylase MACROD1	Protein star
Adenylyl cyclase-associated protein 1	*O*-Acetyl-ADP-ribose deacetylase MACROD2	Pancreatic secretory granule membrane major glycoprotein GP2
Angiopoietin-4	Ornithine carbamoyltransferase	Zinc transporter ZIP10
Ankyrin-2	Palmitoyl-protein thioesterase 1	Serine/threonine-protein kinase unc-51
Band 7 protein AGAP004871	Pancreatic secretory granule membrane major glycoprotein GP2	Chymotrypsin inhibitor
BTB/POZ domain-containing protein 6-A	Peroxidasin-like protein	Clustered mitochondria protein homolog
Calcium-activated potassium channel slowpoke	Phosphoenolpyruvate carboxykinase [GTP]	von Willebrand factor D and EGF domain-containing protein
Calcium-transporting ATPase sarcoplasmic/endoplasmic reticulum type	Phytanoyl-CoA hydroxylase-interacting protein-like	Intermediate filament protein B
Calmodulin	Piwi-like protein 1	Speract receptor
Coiled-coil-helix-coiled-coil-helix domain-containing protein 2	Poly(ADP-ribose) glycohydrolase ARH3	Lombricine kinase
Degenerin unc-8	Polyadenylate-binding protein 1	Synaptogyrin-2
E3 ubiquitin-protein ligase mib1	Probable RNA-directed DNA polymerase from transposon BS	Zinc transporter ZIP4
Exostosin-1c	Protein canopy homolog 2	Caprin-2
FAS-associated factor 2	Protein FADD	Putative uncharacterized transposon-derived protein F54H12,3
Feline leukemia virus subgroup C receptor-related protein 2	Retinal guanylyl cyclase 2	Zinc transporter foi
Fibulin-5	Saccharopine dehydrogenase-like oxidoreductase	4-coumarate--CoA ligase 1
Filamin-C	Sarcoplasmic calcium-binding protein	Mirror-image polydactyly gene 1 protein
Giant hemoglobin linker AV-1 chain	Sodium-coupled monocarboxylate transporter 2	Cell division control protein 6 homolog
Glycoprotein 3-alpha-L-fucosyltransferase A	Sodium/iodide cotransporter	*N*-Lysine methyltransferase SETD8
Heparan sulfate 2-*O*-sulfotransferase 1	Suppressor of G2 allele of SKP1 homolog	ZZ-type zinc finger-containing protein P35G2,11c
Homocysteine-responsive endoplasmic reticulum-resident ubiquitin-like domain member 2 protein	Sushi	Dynamin-2
Immunoglobulin superfamily DCC subclass member 4	Transmembrane protein 127	Serine/threonine-protein phosphatase PGAM5
Interferon-induced guanylate-binding protein 1	Transposable element P transposase	Tyrosine-protein kinase transforming protein SEA
Intermediate filament protein A (fragment)	Trichohyalin	Propionyl-CoA carboxylase alpha chain
Latrophilin Cirl	Tripartite motif-containing protein 2	Calpain-B
Lysenin-related protein 3	tRNA pseudouridine synthase-like 1	WD repeat and HMG-box DNA-binding protein 1
Lysine-specific demethylase 5A	Tuberin	Lachesin
Microtubule-associated protein futsch	Ubiquitin carboxyl-terminal hydrolase 16	Tyrosine-protein kinase Fyn
Mitogen-activated protein kinase kinase kinase 10	Vitamin D 25-hydroxylase	Chromo domain-containing protein cec-1
Mitogen-activated protein kinase kinase kinase 9	Zinc finger protein 140	Acidic mammalian chitinase
NAD(P)H dehydrogenase [quinone] 1	Zinc transporter 1	Acyl-CoA synthetase family member 3
	Zinc/cadmium resistance protein	

Global gene expression profiling indicated a significant overlap in the pathway terms affected by exposure to the two Zn forms. Common term groups included compound binding, Zn homeostasis, and transport, vesicular membrane transport and kinase (see Fig. 2). This high degree of overlap at the pathway level supports our initial hypothesis that the toxic effects of ZnO NPs occur through the same mechanisms as for ionic Zn most likely following ion release from the NPs through dissolution. A common mechanistic effect of ZnO NPs and ionic Zn has been previously indicated for mammals.[58] Our findings are parallel to those by Dekkers *et al.*[27] but instead of using a cell model our observations are based on an environmentally relevant system, involving a whole organism and a chronic exposure. For invertebrates, Poynton *et al.*[28] failed to distinguish between the effects of both Zn forms in a study of gene expression changes in *H. azteca*. In contrast, in *Daphnia magna* Poynton *et al.*[59] suggested a different mode of action, indicating that ZnO NPs affected genes related to reproduction, cellular respiration and cytoskeletal transport. Moreover, Schiavo *et al.*[30] found that distinct apoptosis and antioxidant actions could be attributed to NPs in *M. galloprovincialis.* Hence the degree to which ZnO NPs and ionic Zn share common effects at the pathway level may be species and context (*e.g.* the characteristics of the NPs tested, concentrations, *etc.*) dependent.

In our study with *E. fetida*, the probable common importance of the ions is supported by the common effects seen for both the ZnO NP and ionic Zn on Zn homeostasis and transport. The effects of the Zn handling system were reflected in expression changes of genes encoding several Zn transporters. Cells possess mechanisms for tight control of cytosolic Zn in order to prevent cell death due to Zn toxicity[24] that include two major families of proteins mediating Zn transit across membranes. ZIP transporters increase cytoplasmic Zn concentration by mediating influx through organelles or plasma membrane. ZnT transporters remove Zn from the cytosol out of the cell or into subcellular compartments.[25] Our results show the genetic signatures of this tight control of Zn concentrations. For both the ZnO NPs and ions, the ZIP transporters (ZIP10, ZIP4, ZIP6) were downregulated, whereas ZnT transporters (ZnT1) were upregulated, indicating cellular efforts to eliminate Zn. ZnT1 is the plasma membrane primary regulator of Zn efflux contributing to Zn resistance and playing a large role in regulating free Zn levels.[60] Dietary restriction of Zn has shown upregulation of ZIP4 and downregulation of ZnT1.[61] Here we observed exactly the opposite change under Zn excess. On the other hand, ZIP10 expression has been shown to be downregulated in response to Zn repletion,[62] similarly to our results. Specific for the ZnO NP exposure there was downregulation of ZIP3 and ZIP12 transporters as well as lower gene expression of ZIP10 when compared with the ionic Zn. Hence the ZnO NP exposure specific stronger decrease in transcription of ZIP10 and the other ZIP transporters may indicate a potential difference in Zn supply to cells. Such differences could occur not only through dissolution and mediation with transporters, but also through endocytosis of the undissolved NPs. This implies a necessity to downregulate the major Zn transporters. Known major Zn supporters are predominately located in the plasma membrane. However in addition ZIP3, which is downregulated only for ZnO NPs, is also located in lysosomes, regulating the transport of Zn from this organelle to the cytosol.[63]

Within vesicular/membrane transport category we observed lysosomes and related GO terms were enriched in the NP *vs.* ion comparison. Lysosomes are thought to be targets for NPs accumulation, which may lead to their cellular excretion or most likely chronic lysosome dysfunction.[64] Further vesicular/membrane transport is impacted for both NPs and ions potentially because vesicles are recognized as key for Zn metabolism. For both Zn forms, we observed that membrane-bound vesicle related genes are commonly downregulated (see ESI† File S4), with a higher number of terms enriched for ionic Zn *vs.* control (as shown by Fig. 2 and Table 3). This may be because in the case of NPs, endocytosis is being activated,[9] therefore counteracting this effect on vesicles.

Further GO terms that were significantly enriched as a result of both ZnO NPs and Zn ion exposure were related to activation and regulation of JUN, MAP and JNK kinases. This signaling cascade is known to be a response of a cell to changes in the environment, amplifying and integrating signals from extracellular stimuli and controlling physiological and genomic changes to those.[65] Cellular kinases have previously been shown to be activated by Zn in animals[66] and plants.[67] Protein kinase CK2 was upregulated after the exposure to both forms (>5 fold). It activates ZIP7 through serine phosphorylation, which would result in the release of free ionic Zn in the cytosol and activation of protein kinases involved in cell proliferation, which results in increased cell migration.[25,68] Hence the changes seen in this signaling cascade are consistent with a major mechanism of effects that the result of intracellular organelle level Zn ion exposure.

Zn initially supplied in NP form can potential enter into organism cells either as ions following dissolution in the soil or directly as intact NPs after which they may dissolve rapidly and release ions intracellularly.[69,70] Comparison of the pathway terms indicated that the ZnO NPs cause specific gene expression signatures apart from those related to Zn ion effects, mostly related to GO term that indicates potentially different uptake routes. It has been proposed that active cellular uptake, such as clathrin-mediated endocytosis, maybe a prominent mechanism for the entry of NPs into cells.[71] The size of the presently used NPs (30 nm) is compatible with the sizes reported to enter the endocytic vesicles (10 to 100 nm,[71]). We found clathrin-coated pit to be enriched in NP *vs.* ions comparison supporting this possibility. Moreover, calcium ion binding is enriched for NPs *vs.* ions and control and calcium influx is known to

initiate and accelerate endocytosis.[72] Although it is worth noticing that calcium signaling and modulation of intracellular levels have been linked to NP toxicity.[73,74] Novo *et al.*[9] previously reported endocytosis as a possible uptake route for silver NPs in earthworms and similarly to that study, we found that dynein complex and axoneme related terms are enriched for NPs *vs.* ions. Novo *et al.*[9] hypothesized that the enrichment of those terms could be related to the "ciliary pocket", a basal membrane domain in cilia, involved in clathrin-mediated endocytosis[75] given that earthworms possess ciliated cells in the alimentary epithelia and in several epidermal cell types. Further studies will need to clarify the internalization route of NPs in earthworms and whether it is related to this ciliary pocket. Other studies in invertebrates have also pointed to endocytosis as the uptake route for NPs. Tsyusko *et al.*[76] and González-Moragas *et al.*[77] provided evidence for endocytosis pathways being affected by Gold NPs and iron oxide NPs respectively in *Caenorhabditis elegans* suggesting it as the NPs internalization route.

Zinc influx *via* plasma membrane located ZIP10 and ZIP6 has been established to cause cell-detachment and mobility[78,79] *via* a pathway associated with the normal physiological process linked to Epithelial–mesenchymal transition (EMT). The enrichment of the adhesion term in the ZnO NP exposure compared to ionic Zn suggests that despite the downregulation of ZIP10/ZIP6 there is an enhanced cytosolic release of the zinc ions leading to the trigger of this adhesion pathway. Key to this cascade is alteration in ubiquitin-specific peptidase,[78] which mediates degradation of specific transcription factors controlling expression of factors associated with cell adhesion, and remodeling of the cell environment. It is therefore not surprising that we also observed peptidase and extracellular matrix as terms enriched in gene differentially during exposure to ZnO NPs.

5. Conclusions

ZnO NPs were found to be less toxic compared to ionic Zn, with ionic Zn causing greater effects on survival and reproduction compared to ZnO NPs when exposed at similar soil Zn concentrations, which is in agreement with the majority of findings in similar toxicity studies. Measurements of tissue Zn indicated similar internal concentrations for earthworm experiencing approximately the same degree of reproductive toxicity in both exposures. The critical role of ionic Zn as a key mechanism associated with exposure to both Zn forms was confirmed within a transcriptomic analysis. Common ontology terms linked to Zn homeostasis and transport were commonly affected. The RNA-seq data, however, also identified specific gene expression associated with the ZnO NPs exposure, especially related to vesicular transport and specifically to endocytosis. Furthermore, enrichment analysis of differentially expressed genes associated with ZnO NPs exposure revealed enhanced adhesion and peptidase terms. These processes are linked to a normal physiological function of ionic Zn during epithelial–mesenchymal transition (EMT). The substantial enrichment of the cell adhesion cascade during ZnO NPs exposure suggests NPs facilitate enhanced cellular zinc uptake in a specific manner which triggers this EMT associate processes. This suggested that while the toxicodynamic mechanisms of toxicity for both Zn form may occur through a common mechanism, the pathways of toxicokinetics may differ, with ions taken into cells by ion transporters and ZnO NPs by endocytosis. When in the cell, common gene expression changes highlighted the lysosomal release as a potential common target for any excess accumulated Zn. Overall, our results contribute significantly to the development of adverse outcome pathways for a metal oxide nanomaterial and point to the need to separately consider aspects of both toxicokinetics and toxicodynamics in mechanistic in toxicology studies for nanomaterials.

Conflicts of interest

There are no conflicts to declare.

Acknowledgements

The authors would like to acknowledge the contribution of *the late* Professor A. John Morgan who contributed to experimental design and provided valuable discussions in relation to the interpretation of the data prior to his death. MN and MD were supported by Marie Curie Fellowships, FP7-IEF-GA-2012-329690, FP7-IEF-GA-2010-273207. MN was also supported by a Postdoctoral Fellowship from Complutense University. Remaining authors were supported by NanoFATE, Project-CP-FP-247739 under FP7-NMP-ENV-2009, Theme-4; www. nanofate.eu. DJS and EL were supported by the UKRI IMP scheme project NEC06896.

References

1 A. Laycock, M. Diez-Ortiz, F. Larner, A. Dybowska, D. Spurgeon, E. Valsami-Jones, M. Rehkämper and C. Svendsen, Earthworm Uptake Routes and Rates of Ionic Zn and ZnO Nanoparticles at Realistic Concentrations, Traced Using Stable Isotope Labeling, *Environ. Sci. Technol.*, 2016, **50**, 412–419.

2 M. Diez-Ortiz, E. Lahive, P. Kille, K. Powell, A. J. Morgan, K. Jurkschat, C. A. M. Van Gestel, J. F. W. Mosselmans, C. Svendsen and D. J. Spurgeon, Uptake routes and toxicokinetics of silver nanoparticles and silver ions in the earthworm Lumbricus rubellus, *Environ. Toxicol. Chem.*, 2015, **34**, 2263–2270.

3 S. Makama, J. Piella, A. Undas, W. J. Dimmers, R. Peters, V. F. Puntes and N. W. van den Brink, Properties of silver nanoparticles influencing their uptake in and toxicity to the earthworm Lumbricus rubellus following exposure in soil, *Environ. Pollut.*, 2016, **218**, 870–878.

4 M. Baccaro, A. K. Undas, J. de Vriendt, J. H. J. van den Berg, R. J. B. Peters and N. W. van den Brink, Ageing, dissolution

and biogenic formation of nanoparticles: how do these factors affect the uptake kinetics of silver nanoparticles in earthworms?, *Environ. Sci.: Nano*, 2018, **5**, 1107–1116.

5 L. R. Heggelund, M. Diez-Ortiz, S. Lofts, E. Lahive, K. Jurkschat, J. Wojnarowicz, N. Cedergreen, D. Spurgeon and C. Svendsen, Soil pH effects on the comparative toxicity of dissolved zinc, non-nano and nano ZnO to the earthworm Eisenia fetida, *Nanotoxicology*, 2014, **8**, 559–572.

6 J. E. Cañas, B. Qi, S. Li, J. D. Maul, S. B. Cox, S. Das and M. J. Green, Acute and reproductive toxicity of nano-sized metal oxides (ZnO and TiO2) to earthworms (Eisenia fetida), *J. Environ. Monit.*, 2011, **13**, 3351–3357.

7 S. B. Lovern and R. Klaper, Daphnia magna mortality when exposed to titanium dioxide and fullerene (C60) nanoparticles, *Environ. Toxicol. Chem.*, 2006, **25**, 1132–1137.

8 E. He, H. Qiu, X. Huang, C. A. M. Van Gestel and R. Qiu, Different dynamic accumulation and toxicity of ZnO nanoparticles and ionic Zn in the soil sentinel organism Enchytraeus crypticus, *Environ. Pollut.*, 2019, **245**, 510–518.

9 M. Novo, E. Lahive, M. Diez-Ortiz, M. Matzke, A. J. Morgan, D. J. Spurgeon, C. Svendsen and P. Kille, Different routes, same pathways: Molecular mechanisms under silver ion and nanoparticle exposures in the soil sentinel Eisenia fetida, *Environ. Pollut.*, 2015, **205**, 385–393.

10 C. L. Schultz, A. Wamucho, O. V. Tsyusko, J. M. Unrine, A. Crossley, C. Svendsen and D. J. Spurgeon, Multigenerational exposure to silver ions and silver nanoparticles reveals heightened sensitivity and epigenetic memory in Caenorhabditis elegans, *Proc. Biol. Sci.*, 2016, **283**, 20152911.

11 D. Starnes, J. Unrine, C. Chen, S. Lichtenberg, C. Starnes, C. Svendsen, P. Kille, J. Morgan, Z. E. Baddar, A. Spear, P. Bertsch, K. C. Chen and O. Tsyusko, Toxicogenomic responses of Caenorhabditis elegans to pristine and transformed zinc oxide nanoparticles, *Environ. Pollut.*, 2019, **247**, 917–926.

12 N. W. van den Brink, A. Jemec Kokalj, P. V. Silva, E. Lahive, K. Norrfors, M. Baccaro, Z. Khodaparast, S. Loureiro, D. Drobne, G. Cornelis, S. Lofts, R. D. Handy, C. Svendsen, D. Spurgeon and C. A. M. van Gestel, Tools and rules for modelling uptake and bioaccumulation of nanomaterials in invertebrate organisms, *Environ. Sci.: Nano*, 2019, **6**, 1985–2001.

13 K. Hund-Rinke, K. Schlich, D. Kühnel, B. Hellack, H. Kaminski and C. Nickel, Grouping concept for metal and metal oxide nanomaterials with regard to their ecotoxicological effects on algae, daphnids and fish embryos, *NanoImpact*, 2018, **9**, 52–60.

14 D. A. Notter, D. M. Mitrano and B. Nowack, Are nanosized or dissolved metals more toxic in the environment? A meta-analysis, *Environ. Toxicol. Chem.*, 2014, **33**, 2733–2739.

15 M. Diez-Ortiz, E. Lahive, S. George, A. Ter Schure, C. A. M. Van Gestel, K. Jurkschat, C. Svendsen and D. J. Spurgeon, Short-term soil bioassays may not reveal the full toxicity potential for nanomaterials; bioavailability and toxicity of silver ions (AgNO3) and silver nanoparticles to earthworm Eisenia fetida in long-term aged soils, *Environ. Pollut.*, 2015, **203**, 191–198.

16 A. Romero-Freire, S. Lofts, F. J. Martín Peinado and C. A. M. van Gestel, Effects of aging and soil properties on zinc oxide nanoparticle availability and its ecotoxicological effects to the earthworm Eisenia andrei, *Environ. Toxicol. Chem.*, 2017, **36**, 137–146.

17 G. V. Lowry, A. Avellan and L. M. Gilbertson, Opportunities and challenges for nanotechnology in the agri-tech revolution, *Nat. Nanotechnol.*, 2019, **14**, 517–522.

18 T. M. Benn and P. Westerhoff, Nanoparticle Silver Released into Water from Commercially Available Sock Fabrics, *Environ. Sci. Technol.*, 2008, **42**, 4133–4139.

19 R. Ma, C. Levard, J. D. Judy, J. M. Unrine, M. Durenkamp, B. Martin, B. Jefferson and G. V. Lowry, Fate of Zinc Oxide and Silver Nanoparticles in a Pilot Wastewater Treatment Plant and in Processed Biosolids, *Environ. Sci. Technol.*, 2014, **48**, 104–112.

20 M. Le Bars, S. Legros, C. Levard, P. Chaurand, M. Tella, M. Rovezzi, P. Browne, J. Rose and E. Doelsch, Drastic Change in Zinc Speciation during Anaerobic Digestion and Composting: Instability of Nanosized Zinc Sulfide, *Environ. Sci. Technol.*, 2018, **52**, 12987–12996.

21 M. A. Kiser, P. Westerhoff, T. Benn, Y. Wang, J. Pérez-Rivera and K. Hristovski, Titanium Nanomaterial Removal and Release from Wastewater Treatment Plants, *Environ. Sci. Technol.*, 2009, **43**, 6757–6763.

22 N. C. Mueller and B. Nowack, Exposure Modeling of Engineered Nanoparticles in the Environment, *Environ. Sci. Technol.*, 2008, **42**, 4447–4453.

23 F. Gottschalk, T. Sonderer, R. W. Scholz and B. Nowack, Modeled Environmental Concentrations of Engineered Nanomaterials (TiO2, ZnO, Ag, CNT, Fullerenes) for Different Regions, *Environ. Sci. Technol.*, 2009, **43**, 9216–9222.

24 B. L. Vallee and K. H. Falchuk, The biochemical basis of zinc physiology, *Physiol. Rev.*, 1993, **73**, 79–118.

25 K. M. Taylor, S. Hiscox, R. I. Nicholson, C. Hogstrand and P. Kille, Protein kinase CK2 triggers cytosolic zinc signaling pathways by phosphorylation of zinc channel ZIP7, *Sci. Signaling*, 2012, **5**, ra11.

26 A. Tino, A. Ambrosone, V. Marchesano and C. Tortiglione, Molecular Bases of Nanotoxicology, *Bio- Bioinspired Nanomater.*, 2014, 229–254, DOI: 10.1002/9783527675821.ch09.

27 S. Dekkers, T. D. Williams, J. Zhang, J. Zhou, R. J. Vandebriel, L. J. J. De La Fonteyne, E. R. Gremmer, S. He, E. J. Guggenheim, I. Lynch, F. R. Cassee, W. H. De Jong and M. R. Viant, Multi-omics approaches confirm metal ions mediate the main toxicological pathways of metal-bearing nanoparticles in lung epithelial A549 cells, *Environ. Sci.: Nano*, 2018, **5**, 1506–1517.

28 H. C. Poynton, J. M. Lazorchak, C. A. Impellitteri, B. Blalock, M. E. Smith, K. Struewing, J. Unrine and D. Roose, Toxicity and Transcriptomic Analysis in Hyalella azteca Suggests Increased Exposure and Susceptibility of Epibenthic Organisms to Zinc Oxide Nanoparticles, *Environ. Sci. Technol.*, 2013, **47**, 9453–9460.

29 P. Landa, S. Prerostova, S. Petrova, V. Knirsch, R. Vankova and T. Vanek, The Transcriptomic Response of Arabidopsis thaliana to Zinc Oxide: A Comparison of the Impact of Nanoparticle, Bulk, and Ionic Zinc, *Environ. Sci. Technol.*, 2015, **49**, 14537–14545.

30 J. Li, S. Schiavo, D. Xiangli, G. Rametta, M. L. Miglietta, M. Oliviero, W. Changwen and S. Manzo, Early ecotoxic effects of ZnO nanoparticle chronic exposure in Mytilus galloprovincialis revealed by transcription of apoptosis and antioxidant-related genes, *Ecotoxicology*, 2018, **27**, 369–384.

31 OECD, *OECD 222- Earthworm Reproduction Test (Eisenia fetida/ Eisenia andrei)*.Journal, 2016.

32 E. Lahive, M. Matzke, M. Durenkamp, A. J. Lawlor, S. A. Thacker, M. G. Pereira, D. J. Spurgeon, J. M. Unrine, C. Svendsen and S. Lofts, Sewage sludge treated with metal nanomaterials inhibits earthworm reproduction more strongly than sludge treated with metal metals in bulk/salt forms, *Environ. Sci.: Nano*, 2017, **4**, 78–88.

33 O. Folmer, M. Black, W. Hoeh, R. Lutz and R. Vrijenhoek, DNA primers for amplification of mitochondrial cytochrome c oxidase subunit I from diverse metazoan invertebrates, *Mol. Mar. Biol. Biotechnol.*, 1994, **3**, 294–299.

34 J. D. Thompson, T. J. Gibson, F. Plewniak, F. Jeanmougin and D. G. Higgins, The CLUSTAL_X windows interface: flexible strategies for multiple sequence alignment aided by quality analysis tools, *Nucleic Acids Res.*, 1997, **25**, 4876–4882.

35 P. Villesen, FaBox: an online toolbox for fasta sequences, *Mol. Ecol. Notes*, 2007, **7**, 965–968.

36 B. Langmead, C. Trapnell, M. Pop and S. L. Salzberg, Ultrafast and memory-efficient alignment of short DNA sequences to the human genome, *Genome Biol.*, 2009, **10**, R25–R25.

37 M. D. Robinson, D. J. McCarthy and G. K. Smyth, edgeR: a Bioconductor package for differential expression analysis of digital gene expression data, *Bioinformatics*, 2010, **26**, 139–140.

38 W. Huang da, B. T. Sherman and R. A. Lempicki, Systematic and integrative analysis of large gene lists using DAVID bioinformatics resources, *Nat. Protoc.*, 2009, **4**, 44–57.

39 M. E. Smoot, K. Ono, J. Ruscheinski, P. L. Wang and T. Ideker, Cytoscape 2.8: new features for data integration and network visualization, *Bioinformatics*, 2011, **27**, 431–432.

40 D. Merico, R. Isserlin, O. Stueker, A. Emili and G. D. Bader, Enrichment map: a network-based method for gene-set enrichment visualization and interpretation, *PLoS One*, 2010, **5**, e13984.

41 F. Supek, M. Bosnjak, N. Skunca and T. Smuc, REVIGO summarizes and visualizes long lists of gene ontology terms, *PLoS One*, 2011, **6**, e21800.

42 K. Lock and C. R. Janssen, Modeling zinc toxicity for terrestrial invertebrates, *Environ. Toxicol. Chem.*, 2001, **20**, 1901–1908.

43 D. J. Spurgeon and S. P. Hopkin, Effects of variations of the organic matter content and pH of soils on the availability and toxicity of zinc to the earthworm Eisenia fetida, *Pedobiologia*, 1996, **40**, 80–96.

44 D. J. Spurgeon, C. Svendsen, V. R. Rimmer, S. P. Hopkin and J. M. Weeks, Relative sensitivity of life-cycle and biomarker responses in four earthworm species exposed to zinc, *Environ. Toxicol. Chem.*, 2000, **19**, 1800–1808.

45 D. J. Spurgeon, P. Rowland, G. Ainsworth, P. Rothery, S. Long and H. I. Black, Geographical and pedological drivers of distribution and risks to soil fauna of seven metals (Cd, Cu, Cr, Ni, Pb, V and Zn) in British soils, *Environ. Pollut.*, 2008, **153**, 273–283.

46 R. L. Donnachie, A. C. Johnson, C. Moeckel, M. G. Pereira and J. P. Sumpter, Using risk-ranking of metals to identify which poses the greatest threat to freshwater organisms in the UK, *Environ. Pollut.*, 2014, **194**, 17–23.

47 S. P. Hopkin and C. A. C. Hames, Zinc, among a 'cocktail' of metal pollutants, is responsible for the absence of the terrestrial isopod Porcellio scaber from the vicinity of a primary smelting works, *Ecotoxicology*, 1994, **3**, 68–78.

48 D. J. Spurgeon and S. P. Hopkin, Risk assessment of the threat of secondary poisoning by metals to predators of earthworms in the vicinity of a primary smelting works, *Sci. Total Environ.*, 1996, **187**, 167–183.

49 H. Ma, P. L. Williams and S. A. Diamond, Ecotoxicity of manufactured ZnO nanoparticles–a review, *Environ. Pollut.*, 2013, **172**, 76–85.

50 P. S. Tourinho, C. A. M. van Gestel, S. Lofts, A. M. V. M. Soares and S. Loureiro, Influence of soil pH on the toxicity of zinc oxide nanoparticles to the terrestrial isopod Porcellionides pruinosus, *Environ. Toxicol. Chem.*, 2013, **32**, 2808–2815.

51 P. L. Waalewijn-Kool, M. D. Ortiz, S. Lofts and C. A. M. van Gestel, The effect of pH on the toxicity of zinc oxide nanoparticles to Folsomia candida in amended field soil, *Environ. Toxicol. Chem.*, 2013, **32**, 2349–2355.

52 P. L. Waalewijn-Kool, S. Rupp, S. Lofts, C. Svendsen and C. A. M. van Gestel, Effect of soil organic matter content and pH on the toxicity of ZnO nanoparticles to Folsomia candida, *Ecotoxicol. Environ. Saf.*, 2014, **108**, 9–15.

53 K. Lock and C. R. Janssen, Zinc and cadmium body burdens in terrestrial oligochaetes: Use and significance in environmental risk assessment, *Environ. Toxicol. Chem.*, 2001, **20**, 2067–2072.

54 Z. M. Świątek and A. J. Bednarska, Energy reserves and respiration rate in the earthworm Eisenia andrei after exposure to zinc in nanoparticle or ionic form, *Environ. Sci. Pollut. Res.*, 2019, **26**, 24933–24945.

55 M. Baccaro, A. K. Undas, J. de Vriendt, J. H. J. van den Berg, R. J. B. Peters and N. W. van den Brink, Ageing, dissolution and biogenic formation of nanoparticles: how do these factors affect the uptake kinetics of silver nanoparticles in earthworms?, *Environ. Sci.: Nano*, 2018, **5**, 1107–1116.

56 D. J. Spurgeon and S. P. Hopkin, Comparisons of metal accumulation and excretion kinetics in earthworms (Eisenia fetida) exposed to contaminated field and laboratory soils, *Agric., Ecosyst. Environ., Appl. Soil Ecol.*, 1999, **11**, 227–243.

57 M. G. Vijver, J. P. M. Vink, T. Jager, H. T. Wolterbeek, N. M. van Straalen and C. A. M. van Gestel, Biphasic elimination and uptake kinetics of Zn and Cd in the earthworm Lumbricus rubellus exposed to contaminated floodplain soil, *Soil Biol. Biochem.*, 2005, **37**, 1843–1851.
58 R. J. Vandebriel and W. H. De Jong, A review of mammalian toxicity of ZnO nanoparticles, *Nanotechnol., Sci. Appl.*, 2012, **5**, 61–71.
59 H. C. Poynton, J. M. Lazorchak, C. A. Impellitteri, M. E. Smith, K. Rogers, M. Patra, K. A. Hammer, H. J. Allen and C. D. Vulpe, Differential gene expression in Daphnia magna suggests distinct modes of action and bioavailability for ZnO nanoparticles and Zn ions, *Environ. Sci. Technol.*, 2011, **45**, 762–768.
60 R. D. Palmiter, Protection against zinc toxicity by metallothionein and zinc transporter 1, *Proc. Natl. Acad. Sci. U. S. A.*, 2004, **101**, 4918–4923.
61 R. J. Cousins, J. P. Liuzzi and L. A. Lichten, Mammalian zinc transport, trafficking, and signals, *J. Biol. Chem.*, 2006, **281**, 24085–24089.
62 L. A. Lichten, M. S. Ryu, L. Guo, J. Embury and R. J. Cousins, MTF-1-mediated repression of the zinc transporter Zip10 is alleviated by zinc restriction, *PLoS One*, 2011, **6**, e21526.
63 J. Jeong and D. J. Eide, The SLC39 family of zinc transporters, *Mol. Aspects Med.*, 2013, **34**, 612–619.
64 E. Frohlich, Cellular elimination of nanoparticles, *Environ. Toxicol. Pharmacol.*, 2016, **46**, 90–94.
65 C. R. Weston and R. J. Davis, The JNK signal transduction pathway, *Curr. Opin. Genet. Dev.*, 2002, **12**, 14–21.
66 S. J. Eom, E. Y. Kim, J. E. Lee, H. J. Kang, J. Shim, S. U. Kim, B. J. Gwag and E. J. Choi, Zn(2+) induces stimulation of the c-Jun N-terminal kinase signaling pathway through phosphoinositide 3-Kinase, *Mol. Pharmacol.*, 2001, **59**, 981–986.
67 K. Opdenakker, T. Remans, J. Vangronsveld and A. Cuypers, Mitogen-Activated Protein (MAP) kinases in plant metal stress: regulation and responses in comparison to other biotic and abiotic stresses, *Int. J. Mol. Sci.*, 2012, **13**, 7828–7853.
68 N. A. St-Denis and D. W. Litchfield, Protein kinase CK2 in health and disease: From birth to death: the role of protein kinase CK2 in the regulation of cell proliferation and survival, *Cell. Mol. Life Sci.*, 2009, **66**, 1817–1829.
69 E. J. Park, J. Yi, Y. Kim, K. Choi and K. Park, Silver nanoparticles induce cytotoxicity by a Trojan-horse type mechanism, *Toxicol. In Vitro*, 2010, **24**, 872–878.
70 T. Gomes, J. P. Pinheiro, I. Cancio, C. G. Pereira, C. Cardoso and M. J. Bebianno, Effects of copper nanoparticles exposure in the mussel Mytilus galloprovincialis, *Environ. Sci. Technol.*, 2011, **45**, 9356–9362.
71 G. Sahay, D. Y. Alakhova and A. V. Kabanov, Endocytosis of nanomedicines, *J. Controlled Release*, 2010, **145**, 182–195.
72 X. S. Wu, B. D. McNeil, J. Xu, J. Fan, L. Xue, E. Melicoff, R. Adachi, L. Bai and L. G. Wu, Ca(2+) and calmodulin initiate all forms of endocytosis during depolarization at a nerve terminal, *Nat. Neurosci.*, 2009, **12**, 1003–1010.
73 C. C. Huang, R. S. Aronstam, D. R. Chen and Y. W. Huang, Oxidative stress, calcium homeostasis, and altered gene expression in human lung epithelial cells exposed to ZnO nanoparticles, *Toxicol. In Vitro*, 2010, **24**, 45–55.
74 P. V. Asharani, M. P. Hande and S. Valiyaveettil, Anti-proliferative activity of silver nanoparticles, *BMC Cell Biol.*, 2009, **10**, 65.
75 A. Benmerah, The ciliary pocket, *Curr. Opin. Cell Biol.*, 2013, **25**, 78–84.
76 O. V. Tsyusko, J. M. Unrine, D. Spurgeon, E. Blalock, D. Starnes, M. Tseng, G. Joice and P. M. Bertsch, Toxicogenomic responses of the model organism Caenorhabditis elegans to gold nanoparticles, *Environ. Sci. Technol.*, 2012, **46**, 4115–4124.
77 L. González-Moragas, S. M. Yu, N. Benseny-Cases, S. Sturzenbaum, A. Roig and A. Laromaine, Toxicogenomics of iron oxide nanoparticles in the nematode C. elegans, *Nanotoxicology*, 2017, **11**, 647–657.
78 C. Hogstrand, P. Kille, M. L. Ackland, S. Hiscox and K. M. Taylor, A mechanism for epithelial-mesenchymal transition and anoikis resistance in breast cancer triggered by zinc channel ZIP6 and STAT3 (signal transducer and activator of transcription 3), *Biochem. J.*, 2013, **455**, 229–237.
79 K. M. Taylor, I. A. Muraina, D. Brethour, G. Schmitt-Ulms, T. Nimmanon, S. Ziliotto, P. Kille and C. Hogstrand, Zinc transporter ZIP10 forms a heteromer with ZIP6 which regulates embryonic development and cell migration, *Biochem. J.*, 2016, **473**, 2531–2544.